JOURNAL OF AIRCRAFT
Vol. 34, No. 4, July–August 1997

Design-Oriented Leading-Edge Thrust Force Prediction for Supersonic Lifting Surfaces

Wei-Lin Li* and Eli Livne†
University of Washington, Seattle, Washington 98195

A design-oriented method for evaluating the leading-edge (LE) thrust force on supersonic lifting surfaces with subsonic LE is presented. The method is developed to overcome numerical noise and nonsmooth drag predictions observed when currently attainable LE-thrust techniques are used for wing planform shape optimization. The method is an extension of a design-oriented unsteady supersonic lifting surface capability developed previously for aeroservoelastic shape optimization of wings. It is a panel/lattice method where assumed pressure-weighting functions, taking the LE singularity into account, are prescribed to the LE panels while constant pressure panels are retained elsewhere. Explicit expressions for aerodynamic influence coefficients are retained over most of the wing, except for cases involving the LE panels, where numerical integration must be used. Planform shape sensitivities of the LE thrust and wing pressures are obtained using a combination of analytic and semianalytic techniques. LE thrust force predictions for various configurations are in good agreement with known analytical solutions. Smooth and well-behaved LE thrust force and thrust force sensitivities predictions indicate that this method is suitable for wing-shape design optimization applications based on gradient-based mathematical programming techniques.

Nomenclature

A_{jk} = $(K_0)_{jk}/\sigma_k$
b = reference length
C_T = total thrust force
C_t = thrust force per unit length in spanwise direction
D = design variable
d_j = half-width of the jth panel
$g(y_0)$ = function of chordwise integration
I_{jk} = influence coefficient from LE panel
$(K_0)_{jk}$ = influence coefficient from non-LE panel
M = flight Mach number
N = number of wing panels
q_D = dynamic pressure
R = $\sqrt{x_0^2 - \beta^2 y_0^2}$
t_j = thrust force on the jth LE panel
w = nondimensional downwash
X_{LB}, Y_{LB} = coordinates of the LE break
x_{LE} = LE x coordinate
x_0, y_0 = local coordinates
$x_{0_{LE}}$, x_{0_T} = upper and lower limits of the chordwise integration
α = angle of attack
β = $\sqrt{M^2 - 1}$
Δp = pressure differential of upper and lower surface
$\Delta\tilde{p}$ = coefficient of the LE weighting function
Λ = LE sweep angle
ξ, η = global coordinates
Σ = influence area or integration area for a receiving point
$\bar{\Sigma}$ = $\Sigma - \Sigma_{LE}$
Σ_{LE} = area of LE elements inside Σ
σ_k = area of the kth panel
σ'_k = area of the kth panel inside a Mach cone

Received Aug. 6, 1996; revision received Feb. 20, 1997; accepted for publication Feb. 24, 1997.

*Research Associate, Department of Aeronautics and Astronautics.
†Associate Professor, Department of Aeronautics and Astronautics. Associate Fellow AIAA.

Introduction

THE development and assessment of numerical techniques used to evaluate leading-edge (LE) thrust forces in subsonic and supersonic wing design[1–11] were done in the past from an analysis perspective. That is, convergence, numerical performance, and correlation with test data were the major criteria used for evaluation. The computational efficiency of resulting prediction techniques led to their integration with mathematical programming techniques for the optimization of camber distribution of subsonic and supersonic wings.

When an analysis capability is examined from a design-oriented perspective, however, additional characteristics become important. Speed of computation and accuracy have to be augmented by efficient evaluation of sensitivities with respect to design variables. Availability of intermediate design variables and intermediate response functions becomes important for any approximation-concepts-based optimization.[12,13] Indeed, a design-oriented analysis capability (DOSA) may be quite different in technique, structure, and code organization from a corresponding analysis capability. In the area of structural optimization, this has led to the development of modern structural synthesis tools, such as GENESIS,[14] where sensitivity, approximations, and design considerations had influenced code development from the outset.

The substantial investment over the years in computational analysis tools in many disciplines, and the experience gained with them, led to the development of optimization strategies, in which these tools are used as black boxes.[15,16] This is motivated by the realization that optimization specialists working in the multidisciplinary optimization area (MDO) cannot be in-depth experts in all relevant disciplines. There is a reluctance to invest substantially in the development of new design-oriented analysis tools, and, as new analysis techniques are developed an optimization strategy tailored to the manipulation of black-box tools has the flexibility to replace outdated elements. The growing power of automatic differentiation[17] makes it possible to convert analysis codes to codes that generate analysis and analytic sensitivity information. The moti-

vation to use well-established analysis tools for MDO, rather than redevelop design-oriented new tools, then, only becomes stronger.

To a great extent the success of structural synthesis[12] is owed to the insight its contributors had in the area of structural analysis. It is hard to imagine the discovery of reciprocal approximations, force approximations, and Rayleigh quotient approximations, to mention just a few examples,[13] without in-depth understanding of how structural systems behave, and what characterize the mathematical models used. Any black-box approach, with or without automatically generated analytic sensitivities,[17] faces the risk of missing valuable information, which can affect the automated design process considerably. Without in-depth understanding of the models and computational tools in each discipline involved, it is hard to identify effective intermediate design variables and intermediate response functions, whose utilization can improve approximation accuracy dramatically. Moreover, if noisy predictions are generated by an analysis tool when design variables are varied, and if discontinuous predictions appear, it is hard (without an in-depth look at the analysis and its numerical implementation) to know when these prediction characteristics reflect actual physical behavior of the modeled system and when they are caused by just the numerical approach used.

In recent MDO studies of High Speed Transport (HSCT) configurations[18] it was found that aerodynamic predictions based on the concept of attainable LE thrust[19,20] displayed wavy, nonsmooth behavior when the planform shape of the wing was varied. The waviness seemed to be caused by the numerical solution technique used and not by any real effects. One method of overcoming this difficulty, as pursued in Ref. 18, is by the development of smoothing techniques for the extraction of useful function and sensitivity information out of the noisy data. Indeed, that approach might be helpful with other black-box analysis tools portraying nonsmooth behavior.

In the work described in this paper, an effort was made to overcome the nonsmooth behavior described in Ref. 18. This is motivated by the need to re-examine aerodynamic prediction techniques in the light of design implementation requirements, improve design-oriented features, and gain insight that may lead to the development of accurate approximations based on effective intermediate design variables and response functions in aerodynamics. A similar effort,[21,22] based on the simple formulations of Refs. 23–26, has led to the development of design-oriented analysis and shape-sensitivity capability for unsteady aerodynamics of wings with control surfaces.

In this paper, a method is presented for obtaining an LE thrust–force prediction for supersonic wings subject to planform shape variation, in a way that avoids numerical noise and wavy behavior. Simplicity of formulation and computational speed are pursued as well as reliable sensitivities with respect to shape design variables.

Method Development

The expression of the LE thrust force coefficient is given in Ref. 27 for subsonic lifting surfaces as well as for supersonic wings with subsonic leading edges. In current notations the nondimensional thrust force per unit length in the spanwise direction is expressed as follows:

$$C_t = (\pi/8)\tan\Lambda\sqrt{1-\beta^2\cot^2\Lambda}\cdot(\Delta p\sqrt{x-x_{\mathrm{LE}}})^2\big|_{x\to x_{\mathrm{LE}}} \quad (1)$$

The finite limiting value

$$(\Delta p\sqrt{x-x_{\mathrm{LE}}})\big|_{x\to x_{\mathrm{LE}}} \quad (2)$$

indicates that the singularity of Δp in the vicinity of the leading edge is of the form $1/\sqrt{x-x_{\mathrm{LE}}}$ under the assumption of linearized, small disturbance flow.

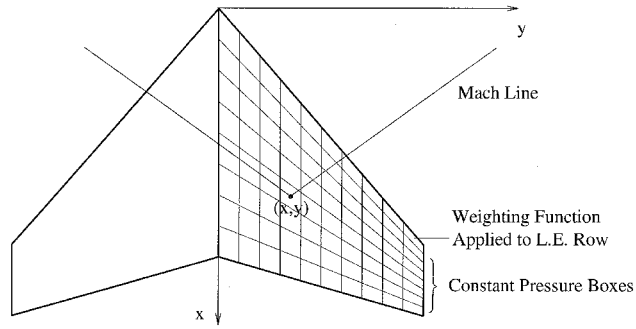

Fig. 1 Pressure-weighting function is assumed for elements in the LE row.

Obviously, the key to accurate evaluation of the theoretical LE thrust force depends on the correct and reliable estimate of this limiting value. Assumed pressure lifting surface solution methods may not yield desirable accuracy, even when the LE singularity is imposed with appropriate weighting functions.[28–31] That is because collocation points, integration formulas, and pressure solutions are usually optimized for minimum error of integral measures such as lift, moment, and other generalized aerodynamic forces, and not the pressure itself. In the case of Mach box methods, the resulting jagged LE introduces pressure fluctuations over the wing. Moreover, for Mach box or other panel methods, curve fitting and extrapolation of pressure distributions in the LE area are required to obtain the limiting value [Eq. (2)], since pressure is usually assumed constant in every element over the wing. The numerical techniques have to rely on empirical correlations with theoretical solutions of linearized flow for simple geometries.[3,32] Variation of aerodynamic panel size may be required in the chordwise direction. When the planform changes shape, these curve-fitting and panel-spacing techniques, as well as inaccuracies in modeling the geometry of the LE, all contribute to fluctuations of the resulting LE thrust force prediction.

LE Weighting Function

In Ref. 21, a lifting surface panel/lattice solution method for supersonic wings has been introduced, based on the acceleration potential formulation. Since the motivation for development arose because of the need to develop analytic aerodynamic sensitivities with respect to planform and control surface shape, aerodynamic influence coefficients in the resulting capability have been expressed explicitly in terms of wing shape design variables, mesh fineness, Mach number, and reduced frequency. These influence coefficients are obtained by area integrations over sending aerodynamic boxes, which may be completely within, or partially within the forward Mach cone of a receiving aerodynamic box.

In the current study, in an effort to capture pressures near the LE more accurately, a weighting function is applied to the row of the LE elements, where the singularity is most influential, while constant pressures are retained for the rest of the elements on the planform (Fig. 1). This means that the theoretical full thrust [via the limiting value, Eq. (2)] and the lift over the wing are obtained from the solutions simultaneously, avoiding curve fitting and extrapolation. Also, because the integration over the area of sending panels is highly accurate, no geometric modeling discontinuities, jagged shape, and resulting fluctuations of the pressure distribution appear.

The analytic solution for pressure distribution on a flat delta wing in linearized supersonic flow for the case of subsonic LE can be obtained from conical flow theory,[33] in nondimensional form, as

$$\Delta p(x,y) = \frac{4\alpha}{E(k')\tan\Lambda\sqrt{1-(y/x)^2\tan^2\Lambda}} \quad (3)$$

where $E(k')$ is the complete elliptic integral of the second kind of modulus k', and $k' = \sqrt{1 - \beta^2 \cot^2\Lambda}$.

Since the solution, Eq. (3), is exact only for delta wings, the common procedure in assumed pressure methods for general configurations employs a series of functions of x and y, multiplied by the singularity of Eq. (3) and other singularities or known pressure behavior, such as along trailing-edge, control-surface hinge lines, and wing-tip pressure variations.[28] In the current approach, the choice of the weighting function is simplified with only the LE elements in consideration. Based on Eq. (3), the weighting function used here for supersonic lifting surfaces with subsonic LEs is

$$\Delta p = \frac{\Delta\tilde{p}}{\sqrt{1 - (x_{\mathrm{LE}}/x)^2}} \tag{4}$$

where x_{LE} is a function of y, and the origin of the $x - y$ coordinates is set in the LE of the wing root. While in all other boxes the unknown pressure is Δp, the unknown in all LE boxes is $\Delta\tilde{p}$.

The integral equation based on the acceleration potential for lifting surfaces in steady supersonic flow is written in the following normalized form for given M:

$$w(x, y) = \frac{1}{8\pi} \int\int_{\Sigma} \Delta p(\xi, \eta) K(x_0, y_0)\, \mathrm{d}\xi\, \mathrm{d}\eta \tag{5}$$

where the integration area Σ is bounded by the forward Mach cone emanating from the receiving point (x, y) and by the edges of the lifting surface. For steady flow, the kernel function is given by

$$K = 2x_0/(Ry_0^2) \tag{6}$$

where

$$\begin{aligned} x_0 &= x - \xi, \qquad y_0 = y - \eta \\ R &= \sqrt{x_0^2 - \beta^2 y_0^2}, \qquad \beta = \sqrt{M^2 - 1} \end{aligned} \tag{7}$$

With the substitution of Eq. (4), the integral relation of Eq. (5) is split into contributions from LE boxes and non-LE boxes, and it is rewritten as

$$8\pi w_j = \sum_{\sigma_k \in \bar{\Sigma}} (K_0)_{jk} \Delta p_k + \sum_{\sigma_k \in \Sigma_{\mathrm{LE}}} I_{jk} \Delta\tilde{p}_k \quad j = 1, 2, \ldots, N \tag{8}$$

$$(K_0)_{jk} = \int\int_{\sigma_k'} \frac{2x_0}{y_0^2 \sqrt{x_0^2 - \beta^2 y_0^2}}\, \mathrm{d}\xi\, \mathrm{d}\eta \tag{9}$$

$$I_{jk} = \int\int_{\sigma_k'} \frac{1}{\sqrt{1 - (\xi_{\mathrm{LE}}/\xi)^2}} \cdot \frac{2x_0}{y_0^2 \sqrt{x_0^2 - \beta^2 y_0^2}}\, \mathrm{d}\xi\, \mathrm{d}\eta \tag{10}$$

The pressures and weighted pressures, Δp_i and $\Delta\tilde{p}_j$, respectively, are unknowns. N is the number of the aerodynamic box elements in the grid system, Σ_{LE} denotes the area of the LE elements inside the forward Mach cone originating at receiving point (x_j, y_j), and $\bar{\Sigma}$ is the rest of the wing surface inside the Mach cone. The downwash (receiving) points are placed at the 95% center chords of all the panels.

While the integrals $(K_0)_{jk}$ can be evaluated analytically with the formulations given in Ref. 21 (for all cases, whether the sending box is completely or partially within the Mach cone), the integrals I_{jk} are evaluated numerically, as shown in the following section.

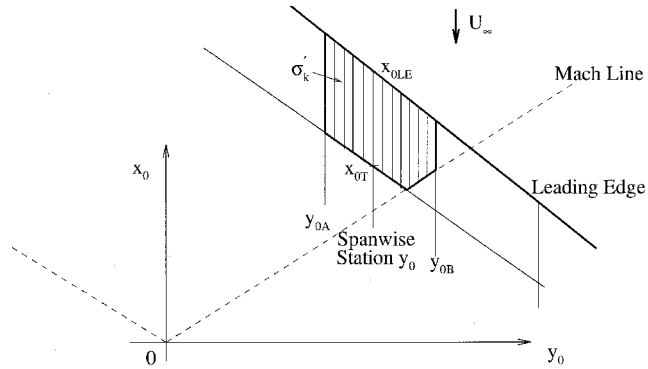

Fig. 2 Integrations in chordwise and spanwise directions in local coordinates.

Numerical Integrations

With numerical integrations in both chordwise and spanwise directions, the integral, Eq. (10), is rewritten as

$$I_{jk} = \int_{y_{0_B}}^{y_{0_A}} \frac{2}{y_0^2}\, g(y_0)\, \mathrm{d}y_0 \tag{11}$$

$$g = \int_{x_{0 \neq y_0}}^{x_{0_{\mathrm{LE}}(y_0)}} \frac{1}{\sqrt{x_{0_{\mathrm{LE}}} - x_0}} \frac{x - x_0}{\sqrt{2x - x_{0_{\mathrm{LE}}} - x_0}} \frac{x_0}{\sqrt{x_0^2 - \beta^2 y_0^2}}\, \mathrm{d}x_0 \tag{12}$$

The integration variables have been changed to the local coordinates, and y_{0_A} and y_{0_B} are the spanwise left and right limits of the integrating area σ_k'. The variable $x_{0_{\mathrm{LE}}}$ is the coordinate of the wing LE, and x_{0_T} is the lower bound in chordwise direction, which may be on the Mach line or the TE of the element, as illustrated in Fig. 2. The chordwise integrations are first calculated to obtain the function $g(y_0)$, at selected spanwise stations y_0 (determined by spanwise integration formulas), before the spanwise integral is carried out to yield the final result of I_{jk}. Integration techniques similar to those described in Ref. 29 are used to evaluate the integrals.

Chordwise integration is carried out with the Tschebycheff–Gaussian quadrature rule for both cases of x_{0_T} being on and not on the Mach line. For the latter case, the integrand of Eq. (12) is not singular at x_{0_T}. Numerical tests showed, however, that overall good accuracy could be achieved for both cases with the same formulation, when 25–30 chordwise integration points were used.

Gaussian quadrature is used in the spanwise integrations with a predetermined number of integration points and tabulated abscissas and weights. In cases when $y_{0_A} > 0$, $y_{0_B} < 0$, a double pole singularity y_0^{-2} appears in the integrand, which occurs when influence coefficients are evaluated because of elements directly upstream of the receiving element, and in the case of calculating the effect of an element on itself. Let the function $g(y_0)$ subtract its Taylor series expansion at $y_0 = 0$, the integral of Eq. (11) then becomes

$$\begin{aligned} I_{jk} = 2 &\int_{y_{0_B}}^{y_{0_A}} \{g(y_0) - [g(0) + g'(0)y_0 + \cdots]\} \frac{\mathrm{d}y_0}{y_0^2} \\ &+ 2 \oint_{y_{0_B}}^{y_{0_A}} [g(0) + g'(0)y_0 + \cdots] \frac{\mathrm{d}y_0}{y_0^2} = I_1 + I_2 \end{aligned} \tag{13}$$

The singularity is moved to the second integral in Eq. (13), and is evaluated analytically in the sense of Mangler's integral[34] to yield the following results.

The first integral I_1 now is regular and can be evaluated numerically with the Gaussian quadrature rule:

$$I_2 = -2g(0) \left(\frac{1}{y_{0_A}} - \frac{1}{y_{0_B}} \right) + 2g'(0)\, \ell n \left| \frac{y_{0_A}}{y_{0_B}} \right| + \cdots \tag{14}$$

Only $g(0)$ and $g'(0)$ terms are kept for the expansion series in Eq. (13), because the other terms are polynomials that can be integrated exactly with Gaussian quadrature formula and would cancel each other with their counterpart in the second integral I_2. The derivative $g'(0)$ is calculated numerically using five-point finite differencing at $y_0 = 0$.

Note, though, that in the case of an LE element influencing itself, the point $x_{0_T} = 0$ moves from the left to the right side of the Mach cone as it crosses $y_0 = 0$. There is a discontinuity if the derivative, as a result $[g'(0^+) \neq g'(0^-)]$. A similar discontinuity may appear if a Mach line cuts a sending box. Using the five-point finite differencing, this discontinuity is smeared and an average value is used. Since the problem occurs in a very small region of the overall integration area for aerodynamic influence coefficients, the effect of this averaging is expected to be small (as, indeed, the accuracy of results indicates). Therefore $g'(0)$ is evaluated in the same way on all LE boxes, whether they are self-inducing or not.

Suction Force

The unknown pressures and LE weighted pressures are found from the system of equations, Eqs. (8), usually using LU decomposition, to yield $\Delta\tilde{p}_j$ for the LE elements and Δp_j for the others. Then the limiting value at jth LE element is obtained as [Eq. (4)]

$$\lim_{x \to x_{\mathrm{LE}}} (\Delta p \sqrt{x - x_{\mathrm{LE}}}) = \sqrt{[(x_{\mathrm{LE}})_j/2]}\Delta\tilde{p}_j \tag{15}$$

where the coordinate of the LE $(x_{\mathrm{LE}})_j$ is evaluated at a spanwise station at the center chord of the element. The thrust force on the jth LE element is calculated from Eq. (1) as

$$\begin{aligned} t_j &= C_t \cdot 2d_j \\ &= (\pi 2d_j/8)\tan\Lambda_j \sqrt{1 - \beta^2 \cot^2\Lambda_j} \cdot \{[(x_{\mathrm{LE}})_j/2](\Delta\tilde{p}_j)^2\} \end{aligned} \tag{16}$$

where d_j is the half-width of the element and Λ_j is local sweep angle. To be consistent with the notation of the supersonic capability in Ref. 21, the thrust force is rewritten as

$$\begin{aligned} t_j &= (\pi/8)d_j(x_{\mathrm{LE}})_j \sqrt{(S_{12})_j^2 - \beta^2} \cdot (\Delta\tilde{p}_j)^2 \\ (S_{12})_j &= \tan\Lambda_j = (x_{01} - x_{02})/(y_{01} - y_{02}) \end{aligned} \tag{17}$$

where subscripts 1, 2 denote the upper two corner points of the jth trapezoidal LE element. The C_T is then obtained by the summation of all the LE panels with thrust force

$$C_T = \sum_j t_j \tag{18}$$

Since all of the variables used in the calculation are normalized, no further reference length and area are assigned to normalize C_t and C_T.

Shape Sensitivity Evaluations

Except for contributions of LE panels, the formulation here is identical to the formulation of Ref. 21, where explicit expressions were obtained, and analytic sensitivities with respect to planform shape presented for the aerodynamic influence coefficients. To obtain analytic sensitivities of the LE panel integrals [Eqs. (11–14)], automatic differentiation could be used. However, supported by satisfactory results in the present study, a semianalytic approach has been adopted, as follows.

The sensitivity of thrust force on jth LE element, with respect to D, is obtained from the differentiation of Eq. (17)

$$\begin{aligned} \frac{\partial t_j}{\partial D} = t_j \Bigg[&\frac{2}{\Delta\tilde{p}_j}\frac{\partial(\Delta\tilde{p}_k)}{\partial D} + \frac{1}{d_j}\frac{\partial d_j}{\partial D} + \frac{1}{(x_{\mathrm{LE}})_j}\frac{\partial(x_{\mathrm{LE}})_j}{\partial D} \\ &+ \frac{(S_{12})_j}{(S_{12})_j^2 - \beta^2}\frac{\partial(S_{12})_j}{\partial D}\Bigg] \end{aligned} \tag{19}$$

The sensitivity of the total thrust can then be calculated with the summation

$$\frac{\partial C_T}{\partial D} = \sum_j \frac{\partial t_j}{\partial D} \tag{20}$$

While the derivatives of d_j, $(x_{\mathrm{LE}})_j$, and $(S_{12})_j$ are explicitly geometry-related and can be calculated analytically, the sensitivities of $\{\Delta\tilde{\boldsymbol{p}}\}$ have to be found d from the aerodynamic equations. The semianalytic method is used in the current study to obtain $\partial\{\Delta\tilde{\boldsymbol{p}}\}/\partial D$ for simplicity.

The following equations result from the differentiation of Eqs. (8), with $\partial f_k/\partial D$ and $\partial(\Delta p_k)/\partial D$ as unknowns:

$$\begin{aligned} &\sum_{\sigma_k \in \bar{\Sigma}} A_{jk}\frac{\partial f_k}{\partial D} + \sum_{\sigma_k \in \Sigma_{\mathrm{LE}}} I_{jk}\frac{\partial(\Delta\tilde{p}_k)}{\partial D} \\ &\quad \approx 8\pi\frac{\partial w_j}{\partial D} - \sum_{\sigma_k \in \Sigma'}\frac{\Delta A_{jk}}{\Delta D}f_k - \sum_{\sigma_k \in \Sigma_{\mathrm{LE}}}\frac{\Delta I_{jk}}{\Delta D}\Delta\tilde{p}_k \\ &\qquad\qquad j = 1, 2, \ldots, N \end{aligned} \tag{21}$$

where

$$\begin{aligned} A_{jk} &= (K_0)_{jk}/\sigma_k \\ f_k &= \Delta p_k \cdot \sigma_k \end{aligned} \tag{22}$$

The notations $\Delta A_{jk}/\Delta D$ and $\Delta I_{jk}/\Delta D$ are used to denote first-order, forward finite difference differentiations, and the vector $\partial\{\boldsymbol{w}\}/\partial D$ is evaluated analytically for given camber distributions.

The solution of the sensitivity problem, Eqs. (21), requires only forward and backward substitution, since the LU-decomposed system matrix is available from the analysis step. After the calculation of $\partial\{\Delta\tilde{\boldsymbol{p}}\}/\partial D$, along with the derivatives of the element half-width $\{\boldsymbol{d}\}$, LE $\{\boldsymbol{x}_{\mathrm{LE}}\}$, and the slope $\{\boldsymbol{S}_{12}\}$, the sensitivities of the LE thrust forces are evaluated with Eqs. (19) and (20). The sensitivities of aerodynamic generalized lifting forces and moments can be obtained simultaneously.

Results and Discussions

To assess the accuracy and reliability of the LE thrust force prediction with the present method, a few numerical calculations for simple planforms are performed and compared with available analytical results. In addition, since the method is aimed at calculating both LE thrust and normal forces over the wing simultaneously, it is important to assess the accuracy of pressure predictions as well. Therefore, test cases are chosen to compare with the results of theoretical analyses as well as results obtained by the supersonic capability developed in Ref. 21, on which the current method was based.

As to the sensitivity analysis, attention is focused on the smoothness of predicted behavior of the thrust force with planform shape variations. As previously discussed in the Introduction, oscillatory predictions would create difficulties in gradient-based optimization. Parametric studies of a swept wing and an HSCT configuration similar to that used in Ref. 18 are presented with thrust force predictions as well as the semianalytic sensitivities with respect to planform shape design variables.

Suction Force Distribution

The significance of the theoretical LE thrust is that it provides a design ideal, as well as the information needed for the evaluations of sustainable LE thrust. The available analytic results from conical flow theory, for flat delta wings[33] and cranked planforms,[35] are used in the following text to compare with the numerical predictions.

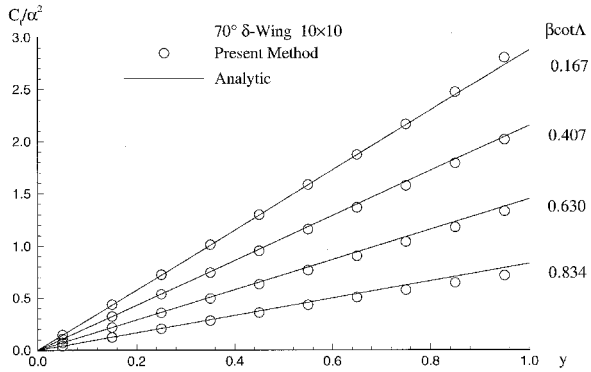

Fig. 3 Numerical LE thrust distributions of a 70-deg sweep delta wing for a range of β cot Λ values, compared with the solutions of conical flow theory. A 10 × 10 mesh is used.

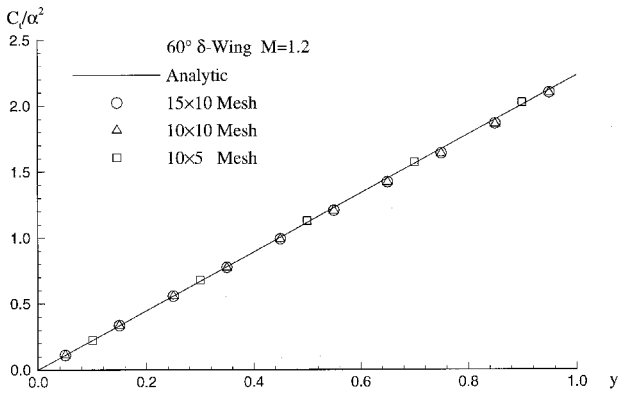

Fig. 4 Comparison of the thrust distributions calculated for various grids of a 60-deg sweep delta wing, at Mach 1.2.

Delta Wings

The analytic solution of conical flow theory, Eq. (3), when $x \to x_{LE}$, gives the limiting value at the LE as

$$\lim_{x \to x_{LE}} (\Delta p \sqrt{x - x_{LE}}) = [2\sqrt{2}\alpha/E(k')]\sqrt{y \cot \Lambda} \tag{23}$$

which, in turn, leads the following linear thrust distribution in the y direction for flat delta wing:

$$C_t = \frac{\pi \alpha^2 \sqrt{1 - \beta^2 \cot^2 \Lambda}}{[E(k')]^2} \cdot y \tag{24}$$

It is seen that, for delta wings normalized with the semispan, LE thrust C_t/α^2 is a function of β cot Λ only. The first group of numerical tests therefore examines the accuracy of the thrust predictions with different values of β cot Λ. Calculations are carried out for the delta wing planform of 70-deg swept angle, and Mach number 1.1, 1.5, 2.0, and 2.5, respectively, corresponding to β cot Λ values 0.167, 0.407, 0.630, and 0.834, on a 10 × 10 uniform mesh. In Fig. 3, the numerical results are shown together with the analytic solutions of Eq. (24), and good agreements are observed over the spectrum of the β cot Λ values.

Additional calculations test the effect of grids on the numerical results. Three sets of uniformly distributed grids, 15 × 10, 10 × 10, and 10 × 5, are used to calculate the LE thrust distribution on a 60-deg sweep delta wing at Mach 1.2 and compare with the conical flow solution in Fig. 4. It appears that results with all different grid sets agree with the analytic solution quite well, a desirable characteristic of the current procedure, especially valuable for planform shape optimizations where the variations of the geometry usually result in changes in panel sizes. High sensitivity of the solutions to grid selection could hinder the convergence of the design optimization process, or give false results.

Cranked Wings

A cranked wing, shown in Fig. 5, consists of two panels of different LE sweep angles Λ_1 and Λ_2. Analytic solutions are given in Ref. 35 for a flat cranked wing, where the inboard panel has subsonic LE (tan $\Lambda_1 > \beta$), and where $\Lambda_1 > \Lambda_2$. The thrust solution on the inboard portion of the LE is the same

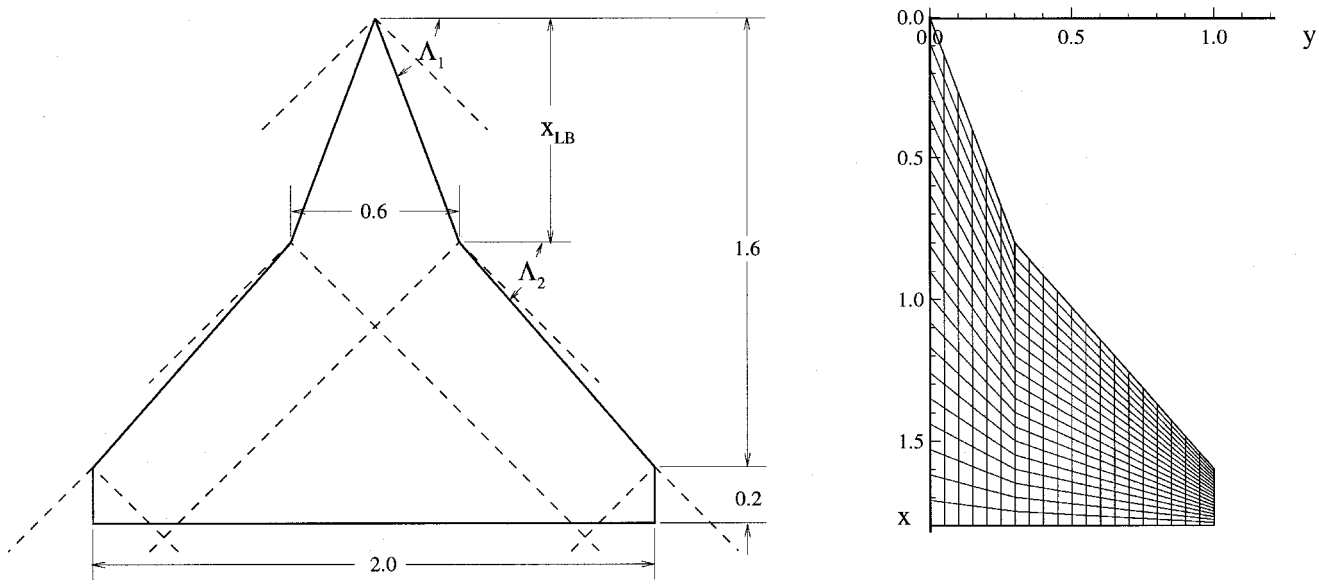

Fig. 5 Cranked planforms and grids for which LE suctions are calculated.

as Eq. (24); whereas the outboard part of the thrust, existing when $\tan \Lambda_2 > \beta$, can be expressed in present notations as

$$C_t = \frac{2\alpha^2}{\pi}\left[\frac{2E(\gamma) - (1-\gamma^2)K(\gamma)}{E(k')}\right]^2 \times \frac{1+m_1}{1+m_2}\sqrt{1-m_2^2}(y + x\cot\Lambda_1) \tag{25}$$

where

$$x = x_{LB} + (y - y_{LB})\tan\Lambda_2$$
$$\gamma = \sqrt{[(1-m_1)(t-m_1)]/[(1+m_1)(t+m_1)]} \tag{26}$$
$$t = \beta(y/x), \qquad m_1 = \beta\cot\Lambda_1, \qquad m_2 = \beta\cot\Lambda_2$$

and (x_{LB}, y_{LB}) are the coordinates of the break point on the LE. The functions $K(\gamma)$ and $E(\gamma)$ are the complete elliptic integrals of the first and second kind of modulus γ.

Numerical calculations are performed for two chosen X_{LB} values of the planform shown in Fig. 5, at Mach 1.2. The numerical thrust prediction for $X_{LB} = 0.65$ ($\Lambda_1 = 65.2$ deg and $\Lambda_2 = 53.6$ deg) on a 10×10 uniform mesh, along with the corresponding analytic solution, are shown in Fig. 6. Two sets of grids, 10×10 and 20×20, are used to calculate the thrust distribution of the wing with $X_{LB} = 0.80$, which has $\Lambda_1 = 69.4$ deg and $\Lambda_2 = 48.8$ deg, and the results are shown in Fig. 7. Good accuracy of the LE thrust can also be achieved in the outer panel of the cranked wing and only slightly different thrust distributions are observed for the coarse and fine grids used.

Pressure Distribution

In addition to the unknown $\{\Delta\tilde{p}\}$ of the LE elements, lifting forces on all other planform surface elements are obtained directly after solving the system of equations [Eq. (8)]. The pressure on the LE element j is then evaluated with the assumed pressure function, Eq. (4), by substituting with the x coordinates on the panel at the half-center-chord x_j, and the center-chord LE $(x_{LE})_j$, i.e.,

$$\Delta p_j = \frac{\Delta\tilde{p}_j}{\sqrt{1 - [(x_{LE})_j/x_j]^2}} \tag{27}$$

Comparisons of pressure distributions with the results of analytic solution and the supersonic capability of Ref. 21 are

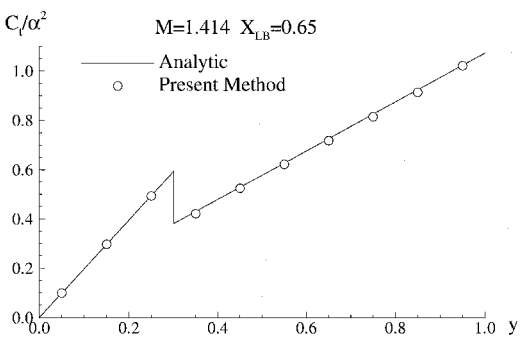

Fig. 6 Comparison of the thrust distributions obtained with the present method and the conical flow solution for the cranked wing of $X_{LB} = 0.65$.

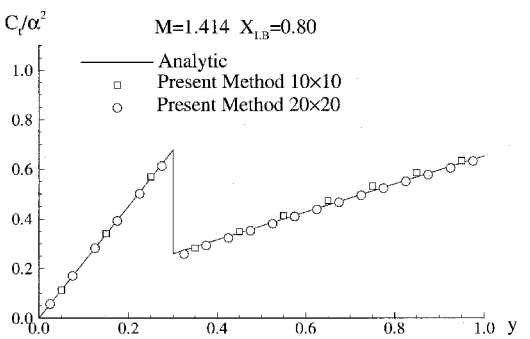

Fig. 7 Comparison of the thrust distributions for the cranked wing of $X_{LB} = 0.80$. 10×10 and 20×20 grids are used for the numerical calculations.

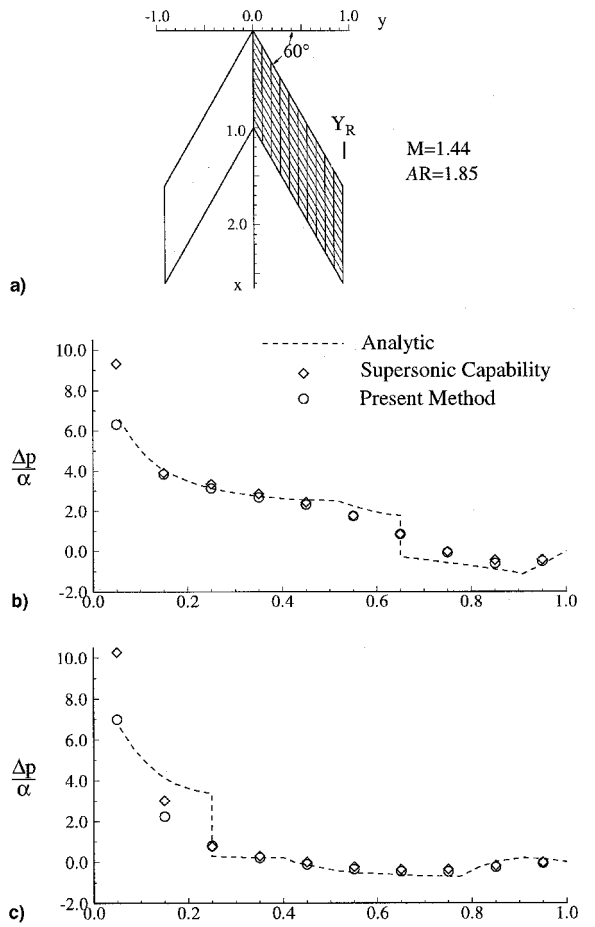

Fig. 8 Comparisons of pressure distributions on the 60-deg constant-chord sweptback wing: a) geometry and grids, b) x/chord at 75% semispan, and c) x/chord at 95% semispan (compared with Ref. 21).

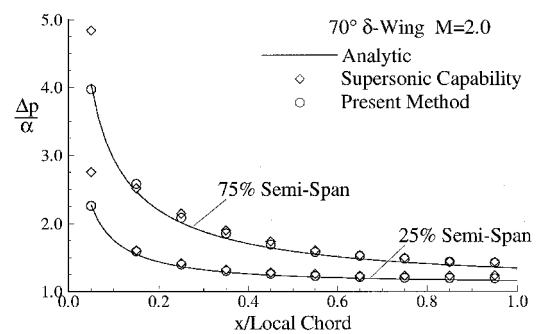

Fig. 9 Comparisons of pressure distributions on a 70-deg delta wing at 25 and 55% of the semispan. 10×10 mesh is used for numerical calculations (compared with Ref. 21).

made for a constant-chord sweptback wing with aspect ratio 1.84 and Mach number 1.44 (Fig. 8a), and a 70-deg sweep delta wing at Mach 2.0. Figures 8 and 9 show that the current method can predict lifting force distribution in good accuracy and the results are close to those of the supersonic capability,[21] with some improvement in the LE vicinity.

Prediction Variations with Respect to Planform Shape

With the gradient-based optimization applications in mind, sensitivities with respect to shape changes are examined for smoothness. In the following calculations, wing root chords are used as length reference scales.

The first test case uses the 60-deg sweptback wing shown in Fig. 8a, at a speed of Mach 1.44. The semispan of the wing is changed from the base design, $Y_R = 0.925-0.740$ (−20% change of the base design), without changing the x locations of the tip chord LE and TE points. This results in a variation of the sweep angle from 60 to 65.2 deg. One-hundred steps are calculated on the Y_R interval [0.740, 0.925] on a 10 × 10 grid, and the total LE C_T and its sensitivity with respect to Y_R are shown in Fig. 10. The step size used for semianalytic sensitivity evaluation is 0.001, whereas the step size of the varying Y_R coordinates is 0.00185. Although some small fluctuations are visible in the sensitivity curve, thrust prediction changes quite smoothly with the variation of the Y_R.

The present work was in part motivated by the report on the oscillatory drag predictions affecting the convergence of an HSCT design process.[18] It is interesting to see how well the current method works when applied to the same problem. A planform similar to the one discussed in Ref. 18, and shown in Fig. 11, is used for the test. At Mach 2.4, calculations are carried out on an uneven 20 × 20 mesh for 200 steps of X_{LB} varying from 0.680 to 0.808, which corresponds to variation

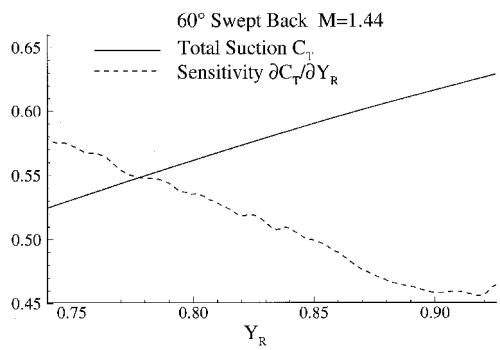

Fig. 10 Variations of the LE thrust and its sensitivity with respect to Y_R vs Y_R for the constant-chord sweptback wing, calculated on a 10 × 10 mesh.

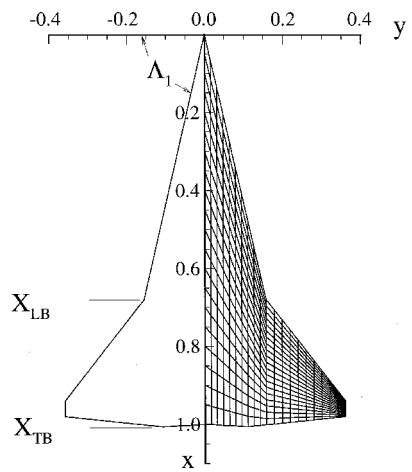

Fig. 11 Geometry of an HSCT planform.

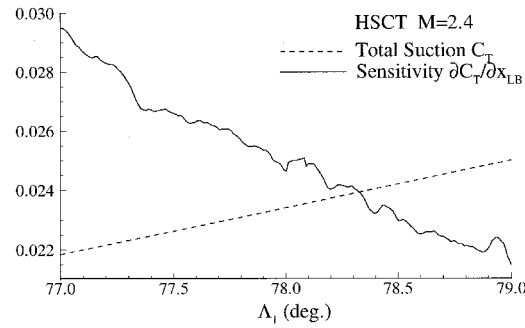

Fig. 12 LE thrust force vs sweep angle for the HSCT planform at Mach 2.4, on a 20 × 20 mesh.

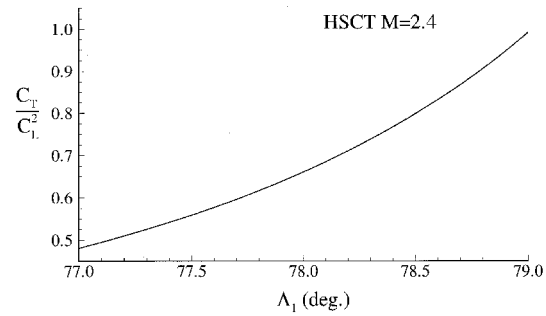

Fig. 13 Variations of the LE thrust and its sensitivity with respect to X_{LB} vs sweep angle for the HSCT planform, calculated on a 20 × 20 mesh.

of the inboard LE sweep angle from 77 to 79 deg. Figure 12 shows the variation of the ratio C_T/C_L^2. No oscillatory behavior was found in the results. Semianalytic sensitivity with respect to X_{LB} is also calculated for step size 0.001 and shown in Fig. 13 along with the variation of the total thrust force. Tests showed that larger step size would smooth out the small oscillations of the sensitivity. However, small fluctuations in sensitivity values, of the order shown in Fig. 13, are not expected to cause any problem in gradient-based optimization. It is nonsmooth functional behavior, leading to large variation in sensitivity, which leads to convergence problems in gradient-based optimization.

Attainable thrust results are not presented in this paper. It is noted that typical empirical formulations, which use the theoretical LE thrust to obtain the attainable thrust, are explicit and continuous in the parameters involved.[3–6] Thus, for planform shape changes, smooth variations of the full thrust force should be expected to result in smooth attainable thrust evaluations.

It should be emphasized here, that, depending on the changes in wing planform and the resulting changes in Mach line patterns over a supersonic wing, there can be situations in which discontinuities in the derivatives of generalized normal loads and thrust forces may appear.[21] The importance of overcoming the numerical noise and wiggly behavior of aerodynamic force prediction by the development of the present capability and of those discussed in Refs. 21 and 22, is that when discontinuities appear, they represent actual behavior of the wing.

Conclusions

To capture the LE singularity, yet to keep the flexibility of panel-type methods for steady/unsteady aerodynamics of general supersonic wing/control surface configurations, an LE weighting function technique is proposed. Design-oriented analysis is pursued in an effort to obtain reliable sensitivity predictions in addition to accurate analysis results. Of special concern is the elimination of numerical noise in the predicted analysis results, reported with existing, widely used supersonic

wing design codes. The current capability yields accurate LE thrust force predictions, accurate normal generalized forces, and accurate, smooth sensitivities with respect to planform shape. It is suitable for applications in gradient-based wing multidisciplinary optimization, without the need for any special processing of its predicted analysis and sensitivity results.

Acknowledgments

This research was supported by NASA Langley Research Center, with Jean-Francois Barthelemy as Grant Monitor. This support is gratefully acknowledged.

References

[1]Polhamus, E. C., "Prediction of Vortex Lift Characteristics by Leading Edge Suction Analogy," *Journal of Aircraft*, Vol. 8, No. 4, 1971, pp. 193–199.

[2]Lamar, J. E., "Subsonic Vortex Flow Design Study for Slender Wings," *Journal of Aircraft*, Vol. 15, No. 9, 1978, pp. 611–617.

[3]Carlson, H. W., and Mack, R. J., "Studies of Leading Edge Thrust Phenomena," *Journal of Aircraft*, Vol. 17, No. 12, 1980, pp. 890–897.

[4]Carlson, H. W., and Walkey, K. B., "Numerical Methods and a Computer Program for Subsonic and Supersonic Aerodynamic Design and Analysis of Wings with Attainable Thrust Considerations," NASA CR-3808, Aug. 1984.

[5]Darden, C., "The Influence of Leading-Edge Load Alleviation on Supersonic Wing Design," *Journal of Aircraft*, Vol. 22, No. 1, 1985, pp. 71–77.

[6]Carlson, H. W., "Survey and Analysis of Research on Supersonic Drag-Due-to-Lift Minimization with Recommendations for Wing Design," NASA TP 3202, Sept. 1992.

[7]Lan, C. E., "A Quasi-Vortex-Lattice Method in Thin Wing Theory," *Journal of Aircraft*, Vol. 11, Sept. 1974, pp. 518–527.

[8]Lan, C. E., "The Unsteady Suction Analogy and Applications," *AIAA Journal*, Vol. 20, Dec. 1982, pp. 1647–1656.

[9]Lan, C. E., and Mehrotra, S. C., "An Improved Woodward's Panel Method for Calculating Leading Edge and Side Edge Suction Forces at Subsonic and Supersonic Speeds," NASA CR-3205, Nov. 1979.

[10]Lan, C. E., and Chang, J.-F., "Calculation of Vortex Lift Effect for Cambered Wings by the Suction Analogy," NASA CR-3449, July 1981.

[11]Lan, C. E., "Applications of CONMIN to Wing Design Optimization with Vortex Flow Effect," NASA CP 2327, Pt. 1, *Recent Experiences in Multidisciplinary Analysis and Optimization*, April 1984.

[12]Schmit, L. A., "Structural Optimization — Some Key Ideas and Insights," *New Directions in Optimum Structural Design*, edited by E. Atrek, R. H. Gallagher, K. M. Ragsdell, and O. C. Zienkiewicz, Wiley, New York, 1984.

[13]Haftka, R. T., and Gurdal, Z., *Elements of Structural Optimization*, 3rd ed., Kluwer Academic, Norwell, MA, 1992, Chap. 6.

[14]"GENESIS," VMA Engineering, Inc., Colorado Springs, CO, March 1995.

[15]Sobieszczanski-Sobieski, J., "Sensitivity of Complex, Internally Coupled Systems," *AIAA Journal*, Vol. 28, No. 1, 1990, pp. 153–160.

[16]Barthelemy, J.-F., Coen, P. G., Wrenn, G. A., Riley, M. F., Dovi, A. R., and Hall, L. E., "Application of Multidisciplinary Optimization Methods to the Design of a Supersonic Transport," NASA TM 104073, March 1991.

[17]Barthelemy, J.-F., and Hall, L. E., "Automatic Differentiation as a Tool in Engineering Design," NASA TM 107661, Aug. 1992.

[18]Giunta, A. A., Dudley, J. M., Narducci, R., Grossman, B., Haftka, R. T., Mason, W. H., and Watson, L. T., "Noisy Aerodynamic Response and Smooth Approximations in HSCT Design," *Proceedings of the AIAA/NASA/USAF/ISSMO Symposium on Multidisciplinary Analysis and Optimization* (Panama City, Fl), AIAA, Washington, DC, 1994.

[19]Mann, M. J., and Carlson, H. W., "Aerodynamic Design of Supersonic Cruise Wings with a Calibrated Linearized Theory," *Journal of Aircraft*, Vol. 31, No. 1, 1994, pp. 35–41.

[20]Carlson, H. W., Mack, R. J., and Barger, R. L., "Estimation of Attainable Leading Edge Thrust for Wings at Subsonic and Supersonic Speeds," NASA TP-1500, Oct. 1979.

[21]Li, W.-L., and Livne, E., "Analytic Sensitivities and Approximations in Supersonic and Subsonic Wing/Control Surface Unsteady Aerodynamics," AIAA Paper 95-1219, April 1995.

[22]Livne, E., and Li, W.-L., "Aeroservoelastic Aspects of Wing/Control Surface Planform Shape Optimization," *AIAA Journal*, Vol. 33, No. 2, 1995, pp. 302–311.

[23]Ueda, T., and Dowell, E. H., "A New Solution Method for Lifting Surfaces in Subsonic Flow," *AIAA Journal*, Vol. 20, No. 3, 1982, pp. 348–355.

[24]Ueda, T., and Dowell, E. H., "Doublet-Point Method for Supersonic Unsteady Lifting Surfaces," *AIAA Journal*, Vol. 22, No. 2, 1984, pp. 179–186.

[25]Roger, K. L., "Airplane Math Modeling Methods for Active Control Design," *Structural Aspects of Active Controls*, CP-228, AGARD, Aug. 1977, pp. 4–11.

[26]Cho, J., and Williams, M. H., "S-Plane Aerodynamics of Nonplanar Lifting Surfaces," *Journal of Aircraft*, Vol. 30, No. 4, 1993, pp. 433–438.

[27]Hayes, W. D., "Linearized Supersonic Flow," Ph.D. Dissertation, California Inst. of Technology, Pasadena, CA, 1947.

[28]Rowe, W. S., "Comparison of Analysis Methods Used in Lifting Surface Theory," *Computational Methods in Potential Aerodynamics*, edited by L. Morino, Springer–Verlag, Berlin, 1986, pp. 197–240.

[29]Cunningham, A. M., Jr., "Oscillatory Supersonic Kernel Function Method for Isolated Wings," *Journal of Aircraft*, Vol. 11, No. 10, 1974, pp. 609–615.

[30]Van Niekerk, B., "Computation of Second Order Accurate Unsteady Aerodynamic Generalized Forces," *AIAA Journal*, Vol. 24, No. 3, 1986, pp. 492–498.

[31]Nissim, E., and Lottati, I., "Supersonic Three Dimensional Oscillatory Piecewise Continuous Kernel Function Method," *Journal of Aircraft*, Vol. 20, No. 8, 1983, pp. 574–681.

[32]Lan, C.-T., and Roskam, J., "Leading-Edge Force Features of the Aerodynamic Finite Element Method," *Journal of Aircraft*, Vol. 9, No. 12, 1972, pp. 864–867.

[33]Stewart, H. J., "The Lift of a Delta Wing at Supersonic Speeds," *Quarterly of Applied Mathematics*, Vol. 4, No. 3, 1946, pp. 246–254.

[34]Ashley, H., and Landahl, M., *Aerodynamics of Wings and Bodies*, Addison–Wesley, Reading, MA, 1965; also Dover, New York, 1985, pp. 132, 133.

[35]Cohen, D., and Friedman, M. D., "Theoretical Investigation of the Supersonic Lift and Drag of Thin, Sweptback Wings with Increased Sweep near the Root," NACA TN 2959, June 1953.